Organic & Biomolecular Chemistry

ROYAL SOCIETY OF CHEMISTRY

PAPER

View Article Online
View Journal

Cite this: DOI: 10.1039/d6ob00309e

Design and synthesis of thiophene-based C_2-symmetric chiral phosphoric acids on a decahydroquinoxaline scaffold for stereoselective transformations

Margherita Gazzotti, †[a] Vincenzo Mirco Abbinante, †[b] Fabrizio Medici, [a] Sara Ghirardi,[b] Sergio Rossi, *[a] Tiziana Benincori, [b] Roberto Cirilli [c] and Maurizio Benaglia *[a]

Received 21st February 2026,
Accepted 31st March 2026

DOI: 10.1039/d6ob00309e

rsc.li/obc

In this study, the design and the synthesis of a thiophene-based phosphoric acid based on a chiral decahydroquinoxaline scaffold derived from enantiopure *trans*-1,2-diaminocyclohexane was reported. This catalyst was then employed in stereoselective transformations such as the enantioselective Friedel–Crafts reaction of indoles with imines to afford 3-indolyl methanamines. High yields (up to 98%) and high enantioselectivities (up to 98% ee) were obtained. DFT calculations were performed to investigate the key transition states, providing mechanistic insight and confirming the origin and sense of the observed stereochemical outcome.

Introduction

Chiral phosphoric acids (CPAs), an important class of chiral Brønsted acids, have been widely employed as organocatalysts in many stereoselective reactions, facilitating the formation of C–C and C–N bonds.[1,2] The remarkable development of CPAs in organic synthesis is primarily attributed to their structural characteristics, which provide precise control over the three-dimensional arrangement of reactants. Chemical activation is enabled by the presence of both a Brønsted acid and Lewis basic sites, while stereochemical control arises from the geometry of the chiral backbone. Such control occurs through the formation of non-covalent interactions with the substrates, including hydrogen bonding, π-stacking, and ion pairing.[3]

Since the early works by Terada[4] and Akiyama,[5] who reported the use of BINOL-derived CPAs in enantioselective reactions, the application of this class of compounds has expanded rapidly in recent years, with numerous studies exploring the various activation models they can adopt: mono activation, dual activation, and bifunctional activation.[6,7] This exceptional adaptability and broad range of activation modes make CPAs a versatile class of catalysts, which has driven the development of numerous chiral phosphoric acid derivatives. Examples of CPAs derived from various chiral backbones, such as BINOL, SPINOL,[8,9] VAPOL,[10] and TADDOL,[11,12] were reported so far, each designed to enhance specific steric or electronic properties, thereby enabling more efficient catalytic reactions.

Despite the success of these CPA derivatives, challenges remain in optimizing their catalytic performance, particularly regarding substrate scope and reaction conditions. Achieving consistent results often demand careful and precise fine-tuning of reaction parameters, even when expanding the substrate scope for the same transformation.[13]

To address some of these challenges, we recently reported a simple synthetic strategy for the synthesis of new CPAs based on a decahydroquinoxaline scaffold where the catalytic site is incorporated into a 9-membered ring (Fig. 1).[14] The exce-

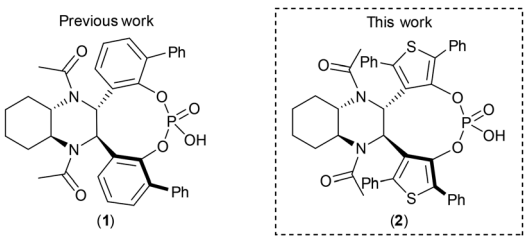

Fig. 1 C_2-Symmetric chiral phosphoric acids on a decahydroquinoxaline scaffold.

[a]*Dipartimento di Chimica, Università degli Studi di Milano, Via Golgi 19, 20133 Milano, Italy. E-mail: maurizio.benaglia@unimi.it, sergio.rossi@unimi.it*
[b]*Dipartimento di Scienza ed Alta Tecnologia dell'Università degli Studi dell'Insubria, Via Valleggio 11, 22100 Como, Italy*
[c]*Dipartimento del Farmaco, Istituto Superiore di Sanità, Viale Regina Elena 299, 00161 Roma, Italy*
† The two authors have equally contributed to the work.

tional chemical and stereochemical efficiency of this novel class of CPAs was demonstrated in the Friedel–Crafts alkylation of indole with *N*-tosylimines,[15] resulting in the formation of the corresponding adducts in high yields and with enantiomeric excesses often exceeding 90%.

To further advance the development of novel CPA structures, we aimed to improve the electron-donating properties of decahydroquinoxaline-based CPAs. Specifically, we hypothesized that replacing the phenyl groups at the 2- and 3-positions of the decahydroquinoxaline core with thiophene rings would affect the stereoelectronic properties of the catalyst, due to the different electronic character of thiophene compared to benzene ring.

Furthermore, the introduction of two phenyl groups at the *ortho* positions relative to the catalytic site would generate the necessary steric hindrance to define the chiral pocket of the catalyst.

Results and discussion

A recently reported methodology efficiently synthesizes decahydroquinoxaline-based CPAs[14] by formation of the chiral backbone by condensation of an aromatic aldehyde with enantiopure *trans*-1,2-diaminocyclohexane, followed by a stereoselective imino–pinacol coupling.[16] Inspired by this strategy, we proposed a comparable approach to synthesize catalyst **2**. The complete synthetic pathway is illustrated in Scheme 1. The synthesis starts from 2,3,5-tribromothiophene **3** which was subjected to the regioselective Suzuki reaction mediated by Pd $(PPh_3)_4$ in a 1 : 1 mixture of THF : H_2O in the presence of Na_2CO_3. The reaction was performed for 24 h and the desired 3-bromo-2,5-diphenylthiophene **4** was obtained in 59% yield.[17] Compound **4** was reacted in a copper catalysed nucleophilic substitution with an excess of sodium methoxide,[18,19] leading to the formation of 3-methoxy-2,5-diphenyl-thiophene **5** in 62% yield. Reaction of **5** with *n*-BuLi in the presence of *N*,*N*,*N*′,*N*′-tetramethyl ethylenediamine (TMEDA), afforded aldehyde (**6**) in 57% yield. Finally, after a treatment of compound **6** with BBr_3 in CH_2Cl_2, aldehyde **7** was formed in quantitative yield. As expected, since hydroxythiophenes are prone to tautomeric equilibrium, the thermodynamically stable ketonic form **7a** of **7** was also observed. The synthesis of the decahydroquinoxaline scaffold was then achieved through a manganese-mediated reductive cyclization of the intermediate **8** obtained by condensation of two molecules of aldehyde **7** with enantiomerically pure (1*S*,2*S*)-*trans*-1,2-diaminocyclohexane yielding (2*R*,2*R*,4a*S*,8a*S*)-**9** in 87% yield.[20]

The same synthetic transformation was performed using (1*R*,2*R*)-*trans*-1,2-diaminocyclohexane and the resulting products were then analyzed and compared using enantioselective HPLC coupled with a circular dichroism detector. This analysis confirmed that the two products, (2*R*,2*R*,4a*S*,8a*S*)-**9** derived from (1*S*,2*S*)-DACH and (2*S*,2*S*,4a*R*,8a*R*)-**9** derived from (1*R*,2*R*)-DACH, are enantiomers, as evidenced by their HPLC traces, which display identical but opposite profiles (Fig. 2). These results clearly highlight that the configuration of the two new stereocenters formed during the pinacol coupling are dictated by the initial configuration of DACH used in the reaction.

In the next step, compound (2*R*,2*R*,4a*S*,8a*S*)-**9** was efficiently protected at the nitrogen atoms as acetyl amides by treating the substrate with an excess of acetyl chloride in the presence of triethylamine. Under these conditions, both NH and OH groups reacted, yielding the tetra-acylated intermediate **10** which was not isolated and directly treated with an excess of $LiBH_4$ in THF to afford desired compound **11** in 76% yield.

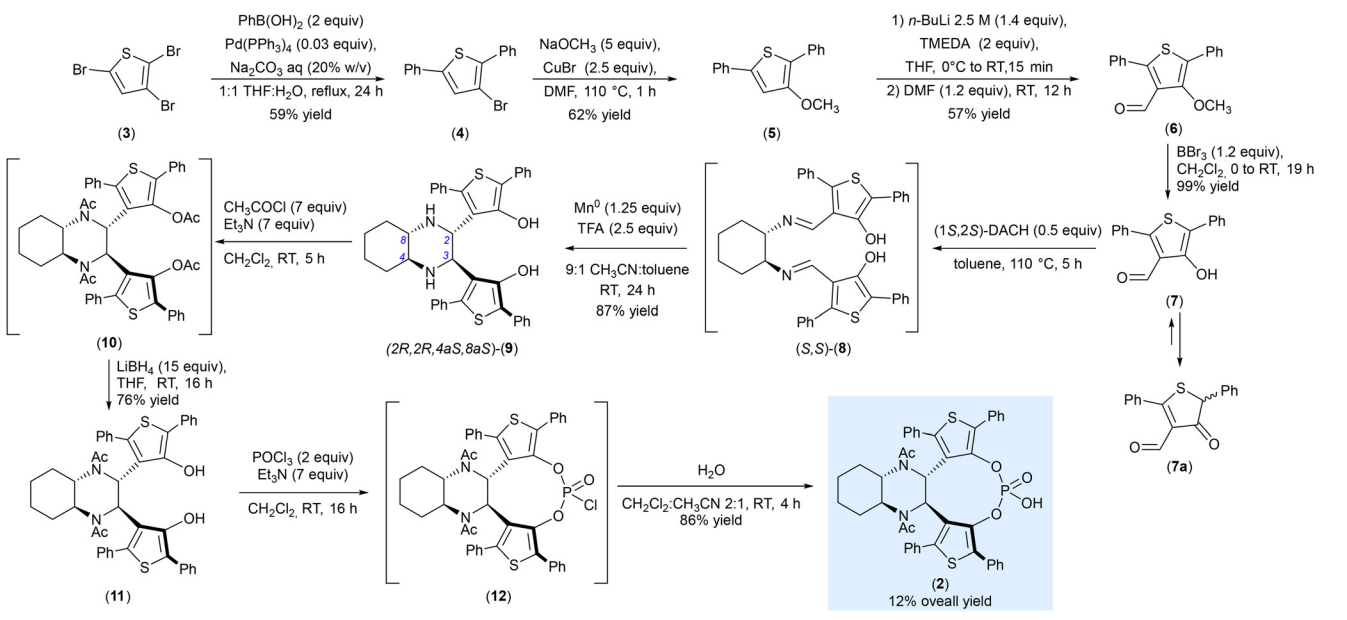

Scheme 1 Synthesis of thiophene-based C_2-symmetric chiral phosphoric acid (**2**) based on a decahydroquinoxaline scaffold.

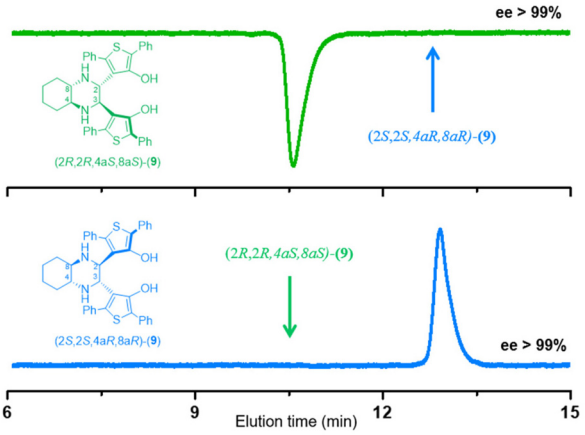

Fig. 2 HPLC assessment of the enantiomeric purity of both enantiomers of compound **9**. Chromatographic conditions: column, Chiralpak IB column (250 mm × 4.6 mm); mobile phase, *n*-hexane/EtOH/DEA (100 : 10 : 0.1); temperature, 40 °C; flow rate, 1.0 mL min^{-1}; detection, CD at 280 nm.

The synthesis of the phosphoric acid **2** was finally achieved by reaction of diol **11** with $POCl_3$ in the presence of Et_3N following a one-pot-two-steps procedure. The intermediate phosphoryl chloride **12**, which was not isolated, was then hydrolysed with water allowing the formation of desired compound **2** in 86% yield. A further treatment with aqueous HCl after chromatographic purification ensures the complete removal of phosphate salts which may be formed during the purification process.[21]

The chemical and stereochemical efficiency of the new chiral Brønsted acid **2** was then investigated in the stereoselective Friedel–Crafts alkylation of indole with *N*-tosyl imines for the synthesis of enantiopure 3-indolyl methanamine derivatives. In a typical experiment, benzaldehyde-derived *N*-tosylimines **13a–c** (1 equiv.) were reacted with indole **14** (5 equiv.) in the presence of 10 mol% of catalyst, operating at −50 °C. Results are reported in Table 1.

When the reaction was performed in toluene, product **15aa** was obtained in 90% yield with 72% ee (entry 1). Notably, replacing toluene with dichloromethane afforded compound **15aa** in almost quantitative yield and 92% ee. With the solvent effect established, the scope of the reaction was subsequently examined. *N*-Tosylimines bearing either electron-withdrawing or electron-donating substituents on the aromatic ring were well tolerated: products **15ba** and **15ca** were obtained in comparable yields with enantioselectivities of 70% ee and 86% ee, respectively (entries 3 and 4). While the difference in enantioselectivity between compound **15aa** and **15ca** is modest (92% *vs.* 86% ee), the more pronounced drop observed for the 4-chloro analogue **15ba** suggests that the aryl substituent on the imine plays a role in determining the stereochemical outcome of the reaction, probably due to some electronic interactions with the aromatic rings of the catalysts.

Table 1 Stereoselective Friedel–Crafts addition of *N*-tosylimines to indoles

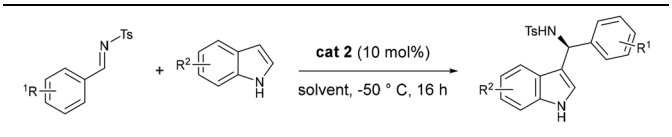

(13a-c) (14a-d) (15aa-ad)

Entry	R^1	R^2	Solvent	Product	Yield (%)	ee (%)
1	H	H	Toluene	**15aa**	90	72
2	H	H	CH_2Cl_2	**15aa**	98	92
3	4-Cl	H	CH_2Cl_2	**15ba**	82	70
4	4-CH_3	H	CH_2Cl_2	**15ca**	84	86
5	H	5-Br	CH_2Cl_2	**15ab**	88	70
6	H	5-Me	CH_2Cl_2	**15ac**	96	98
7	H	5-OMe	CH_2Cl_2	**15ad**	92	93

The substrate scope of the phosphoric acid-catalyzed Friedel–Crafts reaction of indoles with *N*-tosylimines was then further evaluated using substituted indoles bearing either electron-withdrawing or electron-donating groups at the 5-position (entries 5–7). In all cases, the reactions proceeded smoothly to give the corresponding products in high yields and good to excellent enantioselectivities, reaching up to 98% ee when 5-methoxy-1*H*-Indole **14d** was employed (entry 6). In agreement with the trend observed for the imine substituents, electron-donating groups on the indole ring afforded the desired products with higher enantioselectivities, whereas the presence of an electron-withdrawing substituent (as in the case of indole **14a**) resulted in the formation of **15ba** with only 70% ee.

DFT investigation

DFT calculations were employed in order to investigate the steric properties, the Brønsted acidity, and transition-state geometries of the thiophene-based C_2-symmetric chiral phosphoric acid **2** when involved in the Friedel–Crafts alkylation of indole with *N*-tosylimines. Initial conformational geometries were generated through Monte Carlo conformational analysis using molecular mechanics calculations with the OPLS2005 force field,[22] as implemented in the MacroModel package of the Schrödinger suite.[23] These structures were subsequently fully optimized at the DFT level using the M06-2X functional with the 6-31G(d) basis set in Gaussian.[24] Harmonic vibrational frequency calculations were performed at the same level of theory to confirm the nature of the stationary points, ensuring the absence of imaginary frequencies for local minima and the presence of a single imaginary frequency for transition states. The M06-2X functional was selected due to its proven reliability in describing long-range dispersion interactions compared to the B3LYP functional, and its successful application in previous computational studies on chiral phosphoric acids.[14]

The steric properties of the chiral pocket associated to catalyst **2** were evaluated in terms of buried volume (%V_{bur}), a steric parameter that has been successfully employed as a key descriptor for quantifying the fraction of space occupied around the catalytic site.[25]

Compared to the decahydroquinoxaline-based CPA **1**, which has a %V_{bur} of 45.1%, compound **2** exhibits a slightly lower %

V_{bur} value of 40.1% (Fig. 3). Although this corresponds to a slightly larger and more open chiral pocket compared to chiral phosphoric acid **1**, the steric environment of catalyst **2** remains within the range characteristic of high-performing phosphoric acids, providing a spatial confinement able to influence the substrate orientation and to promote enantioselective control; as demonstrated by the stereochemical outcome observed in the Friedel–Crafts alkylation of indole with *N*-tosylimines. Notably, this value is comparable to that of the SPINOL-derived phosphoric acid (%V_{bur} = 41.1%) and significantly higher than that of the BINOL-derived analogue, which displays a %V_{bur} of 33%.[14]

Moreover, dedicated computational studies performed to determine the acidity of catalyst **2**. Two complementary approaches were employed: the isodesmic method,[26] computed at M06-2X/6-31G(d) level of theory, and the linear free energy solvation relationship (LFESR) model,[27] performed at the M06-2X/6-311++G(d,p) level with the SMD(DMSO) solvation model. The results indicate a corrected p$K_{a(isodesmic)}$ in DMSO of 1.00, whereas the LFESR approach yielded slightly higher values of 1.36 in DMSO (p$K_{a(LFESR)}$ CH_3CN = 10.99). Overall, the two methods provide consistent trends, confirming the relatively strong Brønsted acidity of catalyst **2** compared to catalyst **1** (p$K_{a(isodesmic)}$ DMSO = 3.97). At the present it is premature to offer a rationalization of this observation, since several factors are likely contributing to the pK_a value. Although thiophene is generally considered as an electron-rich heterocycle, it must be noted that sulfur atom is more polarizable than carbon atom, and the 5-membered thiophene rings lead to a larger chiral pocket (see Fig. 3), where the conjugate base of catalyst **2** will be accommodated, and may experience stereoelectronic interactions with other aryl rings that may affect the negative charge stabilization.

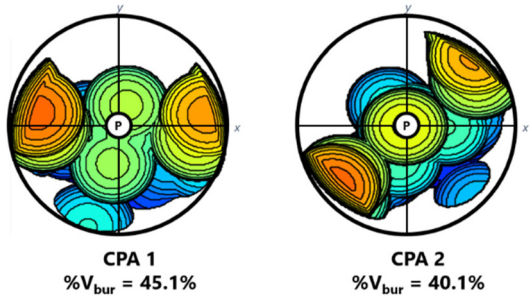

Fig. 3 Steric maps based on DFT-optimized CPAs structures viewed down the *z*-axis. %V_{bur} was determined using a 4.5 Å radius coordination sphere, whose center was displaced by 2.0 Å along the *z*-axis from the phosphorus atom (the red and the blue zones indicate the more and the less-hindered zones in the catalytic pocket, respectively).

After the steric properties of the chiral pocket and the Brønsted acidity of the catalyst were characterized, the origin of stereoselectivity in the enantioselective addition of indoles to *N*-tosylimines catalyzed by chiral phosphoric acid **2** was investigated. In this transformation, CPAs are known to operate through a bifunctional activation mechanism, in which the imine is activated *via* hydrogen bonding to the Lewis basic site, thereby polarizing the C=N bond and increasing its electrophilicity, while the NH group of the indole forms a hydrogen bond with the Brønsted site of the catalyst, aligning the nucleophilic C3 of the indole for enantioselective attack.[8,28]

Although decahydroquinoxaline-based CPAs feature an additional amidic functionality, allowing several possible coordination modes, the classical model has been shown to be energetically preferred.[14] For this reason, only this coordination mode was considered in this computational study. In Fig. 4 the transition states corresponding to eight possible conformers are reported.

DFT calculations indicate that transition states in which the imine adopts the *E* configuration are consistently more stable than those involving the *Z* configuration. In particular, **TS3-*E*-*endo*-(*S*)**, leading to the experimentally observed (*S*)-**15aa** product,

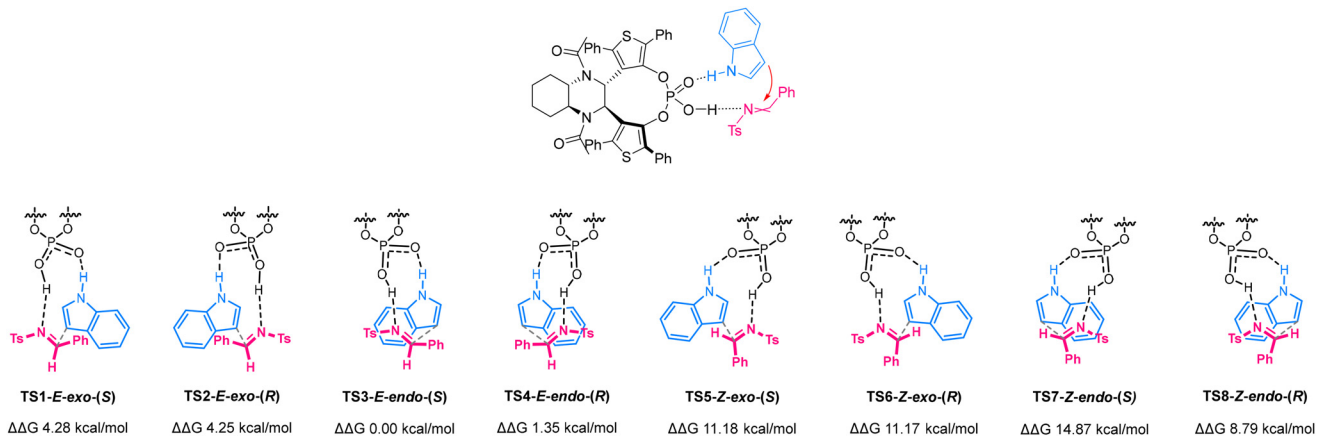

Fig. 4 Computed transition states for the Friedel–Crafts addition of *N*-tosylimine (**13a**) to indole (**14a**). The *E* and *Z* in the names refer to the configuration of the imine double bond, whereas the (*R*) and (*S*) description refers to the final configuration of product (**15aa**). In the competing conformations for the transition states, decahydroquinoxaline scaffold omitted for clarity; ΔΔ*G* values (*in vacuo*) are expressed in kcal mol^{-1} and calculated at M06-2X/6-311G(++)(2d,2p)//M06-2X/6-31G(d) level of theory.

is calculated to be 1.35 kcal mol^{-1} lower in energy than **TS4-*E*-*endo*-(*R*)**. Interestingly, in contrast to traditional CPAs based on the decahydroquinoxaline scaffold, the new C–C bond formation occurs according to an *endo* orientation, in which the imine C═N bond superimposes with the five-membered ring of the indole, likely as a result of improved accommodation within a less sterically congested chiral pocket of the catalyst.

Gibbs free energies computed a M06-2X/6-311G(++)(2d,2p) PCM (dichloromethane)//M06-2X/6-31G(d) were used to estimate an enantiomeric excess of 91% in favour of the (*S*)-**15aa** enantiomer for catalyst **2** at −50 °C in DCM. The ee was calculated using the Eyring equation, relating the relative free energies of the transition states to the corresponding rate constants. This theoretical prediction is in perfect agreement with the experimentally observed enantioselectivity of 92% obtained under the same conditions.

Conclusions

In this work, we have developed a new example of chiral phosphoric acid based on a decahydroquinoxaline scaffold[29] which incorporates two thiophene rings.

The chiral backbone was synthesized through the condensation of aldehyde **7** with enantiopure *trans*-1,2-diaminocyclohexane **6**, followed by a stereoselective intramolecular pinacol coupling. The optical purity of a key intermediate **9** was confirmed through HPLC analysis with a CD detector.

The catalytic performance of the resulting CPA was evaluated in the stereoselective Friedel–Crafts alkylation of indole with *N*-tosylimines, resulting in the formation of the desired products with yields up to 96% and up to 98% enantiomeric excesses. DFT calculations further showed that the transition state leading to the experimentally observed (*S*)-product is lower in energy than that of the competing (*R*)-pathway, in line with the observed experimental data. Gibbs free energies computed for all relevant transition states were used to estimate the enantiomeric excess, yielding a value in good agreement with the experimental results.

These findings demonstrate that the new CPA exhibits both high catalytic activity and predictable stereocontrol. Ongoing studies are focused on further optimizing catalyst structure and exploring the application of these catalysts in additional stereoselective transformations to expand their utility in synthetic organic chemistry.

Conflicts of interest

There are no conflicts to declare.

Data availability

The data supporting this article have been included as part of the supplementary information (SI). Computational data presented in the study are openly available in Dataverse UNIMI at: https://doi.org/10.13130/RD_UNIMI/SVQMPB.

Supplementary information is available. See DOI: https://doi.org/10.1039/d6ob00309e.

Acknowledgements

S. Rossi and M. Benaglia thank MUSA – Multilayered Urban Sustainability Action – project, funded by the European Union – NextGenerationEU, under the National Recovery and Resilience Plan (NRRP) Mission 4 Component 2 Investment Line 1.5: Strengthening of research structures and creation of R&D "innovation ecosystems", set up of "territorial leaders in R&D". S. Rossi thanks MUR for the project PRIN 2022 "Enabling technologies for sustainable and innovative catalytic transformations – BEST-CAT" (CUP G53D23003260006) and University of Milan grant PSR2025 "Catalytic approaches to the sustainable synthesis of high added-value fine chemicals. M. Gazzotti thanks University of Milan for a PhD fellowship.

S. Rossi, M. Benaglia and T. Benincori thank Project 6154644 – GREEN-TECH of Regione Lombardia (Bando collabora e Innova).

Computational studies were performed using INDACO Platform, which is a project of High Performance Computing at the University of Milan. Mass spectrometry analyses were performed at the MS facility of the Unitech COSPECT at the University of Milan (Italy). Scientific support from CRIETT centre of University of Insubria (instrument code: MAC01, MAC15) is greatly acknowledged.

References

1 A. G. Woldegiorgis, Z. Han and X. Lin, *J. Mol. Struct.*, 2024, **1297**, 136919.
2 E. I. Jimenez, *Org. Biomol. Chem.*, 2023, **21**, 3477–3502.
3 X. del Corte, E. Martínez de Marigorta, F. Palacios, J. Vicario and A. Maestro, *Org. Chem. Front.*, 2022, **9**, 6331–6399.
4 D. Uraguchi and M. Terada, *J. Am. Chem. Soc.*, 2004, **126**, 5356–5357.
5 T. Akiyama, J. Itoh, K. Yokota and K. Fuchibe, *Angew. Chem., Int. Ed.*, 2004, **43**, 1566–1568.
6 R. Maji, S. C. Mallojjala and S. E. Wheeler, *Chem. Soc. Rev.*, 2018, **47**, 1142–1158.
7 D. Parmar, E. Sugiono, S. Raja and M. Rueping, *Chem. Rev.*, 2014, **114**, 9047–9153.
8 F. Xu, D. Huang, C. Han, W. Shen, X. Lin and Y. Wang, *J. Org. Chem.*, 2010, **75**, 8677–8680.
9 A. Rahman and X. Lin, *Org. Biomol. Chem.*, 2018, **16**, 4753–4777.
10 W. Wulff and A. Desai, *Synthesis*, 2010, 3670–3680.
11 T. Akiyama, Y. Saitoh, H. Morita and K. Fuchibe, *Adv. Synth. Catal.*, 2005, **347**, 1523–1526.
12 A. Voituriez and A. B. Charette, *Adv. Synth. Catal.*, 2006, **348**, 2363–2370.

13 J. P. Reid and J. M. Goodman, *Chemistry*, 2017, **23**, 14248–14260.
14 M. Gazzotti, M. Orlandi, S. Rossi, L. Raimondi and M. Benaglia, *ChemistryEurope*, 2025, 202500234.
15 Q. Kang, Z-A. Zhao and S-L. You, *J. Am. Chem. Soc.*, 2007, **129**(6), 1484–1485.
16 For a electrochemical stereoselective imino pinacol coupling see: ; M. Gazzotti, F. Medici, V. Chiroli, L. Raimondi, S. Rossi and M. Benaglia, *Beilstein J. Org. Chem.*, 2025, **21**, 1897–1908; See also; F. Medici, S. Resta, A. Puglisi, S. Rossi, L. Raimondi and M. Benaglia, *Molecules*, 2021, **26**(22), 6968.
17 S. Gabrieli, R. Cirilli, T. Benincori, M. Pierini, S. Rizzo and S. Rossi, *Eur. J. Org. Chem.*, 2017, 861–870.
18 M. A. Keegstra, T. H. A. Peters and L. Brandsma, *Tetrahedron*, 1992, **48**, 3633–3652.
19 L. D. Peeters, S. G. Jacobs, W. Eevers and H. J. Geise, *Tetrahedron*, 1994, **50**, 11533–11540.
20 G. J. Mercer and M. S. Sigman, *Org. Lett.*, 2003, **5**, 1591–1594.
21 B. List, M. Klussmann, L. Ratjen, S. Hoffmann, V. Wakchaure and R. Goddard, *Synlett*, 2010, 2189–2192.
22 C. Lu, C. Wu, D. Ghoreishi, W. Chen, L. Wang, W. Damm, G. A. Ross, M. K. Dahlgren, E. Russell, C. D. Von Bargen, R. Abel, R. A. Friesner and E. D. Harder, *J. Chem. Theory Comput.*, 2021, **17**, 4291–4300.
23 *Schrödinger Release 2024-1: MacroModel*, Schrödinger, LLC, New York, NY, 2024.
24 M. J. Frisch, G. W. Trucks, H. B. Schlegel, G. E. Scuseria, M. A. Robb, J. R. Cheeseman, G. Scalmani, V. Barone, G. A. Petersson, H. Nakatsuji, X. Li, M. Caricato, A. V. Marenich, J. Bloino, B. G. Janesko, R. Gomperts, B. Mennucci, H. P. Hratchian, J. V. Ortiz, A. F. Izmaylov, J. L. Sonnenberg, D. Williams-Young, F. Ding, F. Lipparini, F. Egidi, J. Goings, B. Peng, A. Petrone, T. Henderson, D. Ranasinghe, V. G. Zakrzewski, J. Gao, N. Rega, G. Zheng, W. Liang, M. Hada, M. Ehara, K. Toyota, R. Fukuda, J. Hasegawa, M. Ishida, T. Nakajima, Y. Honda, O. Kitao, H. Nakai, T. Vreven, K. Throssell, J. A. Montgomery, Jr., J. E. Peralta, F. Ogliaro, M. J. Bearpark, J. J. Heyd, E. N. Brothers, K. N. Kudin, V. N. Staroverov, T. A. Keith, R. Kobayashi, J. Normand, K. Raghavachari, A. P. Rendell, J. C. Burant, S. S. Iyengar, J. Tomasi, M. Cossi, J. M. Millam, M. Klene, C. Adamo, R. Cammi, J. W. Ochterski, R. L. Martin, K. Morokuma, O. Farkas, J. B. Foresman and D. J. Fox, *Gaussian 16, Revision C.01*, Gaussian, Inc., Wallingford CT, 2019.
25 A. Poater, B. Cosenza, A. Correa, S. Giudice, F. Ragone, V. Scarano and L. Cavallo, *Eur. J. Inorg. Chem.*, 2009, 1759–1766.
26 C. Yang, X. S. Xue, J. L. Jin, X. Li and J. P. Cheng, *J. Org. Chem.*, 2013, **78**, 7076–7085.
27 M. Busch, E. Ahlberg, E. Ahlberg and K. Laasonen, *ACS Omega*, 2022, **7**, 17369–17383.
28 L. Simon and J. M. Goodman, *J. Org. Chem.*, 2010, **75**, 589–597.
29 For the use of chiral decahydroquinoxaline-based phosphoroamidite see: ; B. Zhao, Z. Wang and K. Ding, *Adv. Synth. Catal.*, 2006, **348**, 1049–1057.